Available online at www.sciencedirect.com
ScienceDirect
International Journal of Multiphase Flow 33 (2007) 1172–1185
International Journal of Multiphase Flow
www.elsevier.com/locate/ijmulflow

Microgravity flow regime data and analysis

Luca Valota [a,*], Cable Kurwitz [a], Adam Shephard [a], Frederick Best [a,b]

[a] Department of Nuclear Engineering, Texas A&M University, College Station, TX 77843, United States
[b] NASA Center for Space Power, Texas A&M University, College Station, TX 77843, United States

Received 7 April 2006; received in revised form 7 March 2007

Abstract

To utilize the advantageous properties of two-phase flow in microgravity applications, the knowledge base of two-phase flow phenomena must be extended to include the effects of gravity. In the experiment described, data regarding the behavior of two-phase flow in a conduit under microgravity conditions (essentially zero gravity) are explored. Of particular interest, knowledge of the void fraction of the gas and liquid in a conduit is necessary to develop models for heat and mass transfer, pressure drop, and wall shear. An experiment was conducted under reduced gravity conditions to collect data by means of a capacitance void fraction sensor and high speed visual imagery. Independent parameters were varied to map the flow regime regions. These independent parameters include gas and liquid volumetric flow rates and saturation pressures. Void fraction measurements were taken at a rate of 100 Hz with six sensors at two locations along the conduit. Further, statistical parameters were developed from the void fraction measurements. Statistical parameters such as variance, signal-to-noise ratio, half height value, and linear area difference were calculated and found to have characteristics allowing flow regime identification.

Keywords: Two-phase; Microgravity; Separator; Void fraction; Flow regime; Multiphase flow

1. Introduction

The advantages of actively pumped two-phase systems over single-phase systems have yet to be exploited in current space programs primarily due to the underdevelopment of the microgravity two-phase knowledge base. The general technology readiness level (TRL) is estimated to be in the 4–6 range depending on the particular application even though two-phase flow systems have been operationally deployed. In comparison with single-phase flow, two-phase flow carries more energy per fluid unit mass, operates at near constant temperature, requires less pumping power per unit mass thermal energy carried, and has better heat transfer characteristics (Hill and Best, 1991). The reductions in volume, mass, and power result in higher system efficiencies and performance compared to equivalent single-phase systems (Ungar, 1995). Reliable design of such systems

* Corresponding author. Tel.: +1 979 845 4108.
E-mail addresses: l_valota@hotmail.com (L. Valota), kurwitz@tamu.edu (C. Kurwitz), shephard@tamu.edu (A. Shephard), fbest@tamu.edu (F. Best).

0301-9322/$ - see front matter © 2007 Elsevier Ltd. All rights reserved.
doi:10.1016/j.ijmultiphaseflow.2007.03.002

requires an understanding of microgravity two-phase phenomena that is yet to be obtained. At this time, a complete theoretical scheme for the behavior of microgravity two-phase flow has not been developed. Consequently, we use approximate theory or correlations applicable under restrictive conditions. Limitations in the developments surrounding microgravity two-phase research stem from the constraints of the microgravity laboratory. Currently, experimentation is preformed in microgravity aboard spacecraft such as the shuttle, sounding rockets, or aboard terrestrial aircraft or drop towers. Reduced gravity aircraft climb and dive repetitiously, following a partial elliptical path to provide periods of 1.8 g and 0 g. Difficulties lie in the short duration of microgravity conditions. The short duration constricts the range of achievable experimental conditions and reduces the range of application for empirical models.

2. Background

Two-phase flow regimes are dependent upon a multitude of parameters. Phase velocity, density, viscosity, and surface tension are thought to play a role in determining the flow regime. Traditionally, two-phase flow regimes are classified based on the spatial orientation of gas and liquid shown in Fig. 1 (Reinarts, 1993).

Note that flow regime identification is somewhat subjective since it is determined visually by the experimenter (Elbow and Rezkallah, 1997; Reinarts, 1993; Janicot and Dukler, 1993). Empirical models have been developed that can identify the flow regime given system parameters. Usually all the parameters of the system are necessary in order to predict which flow regime will occur. However, in the present work, a method to identify the flow pattern using only the void fraction measurement is analyzed. Specifically, the fluctuations in the void fraction measurement are the key in identifying the flow regime.

Jones and Zuber (1975) were the first to apply the statistical examination of fluctuations of the void fraction for flow pattern identification. They used a fast response X-ray void fraction measurement system of air–water in a rectangular channel. They concluded that the flow regime can indeed be identified by statistical analysis of void fraction fluctuations.

Vince and Lahey (1982) used an X-ray system similar to Jones and Zuber (1975) to make chordal-average void fraction measurements. This experimental apparatus provided more accurate findings than Jones and Zuber (1975). Additionally, the first four statistical moments associated with the void fraction measurements were investigated as flow regime identifiers. Vince and Lahey concluded that the moments indicated various flow regime transitions and thus could be used as flow regime identifiers.

Various methods have been developed to measure void fraction in a system including quick-closing valves (Chang, 1997), neutron scattering, optical probes, gamma-ray and X-ray absorption, hot-film anemometry, and impedance methods using conductance probes or capacitance probes (Chang, 1997; Lowe and Rezkallah, 1999; Crowley et al., 1996). The present experiment takes advantage of the CREARE Inc. Capacitance Void Fraction Sensor (Crowley et al., 1996). It is an order of magnitude more accurate than the void fraction sensors used in both Jones and Zuber (1975) and Vince and Lahey (1982). New statistical parameters will be introduced to evaluate flow regime identifiers.

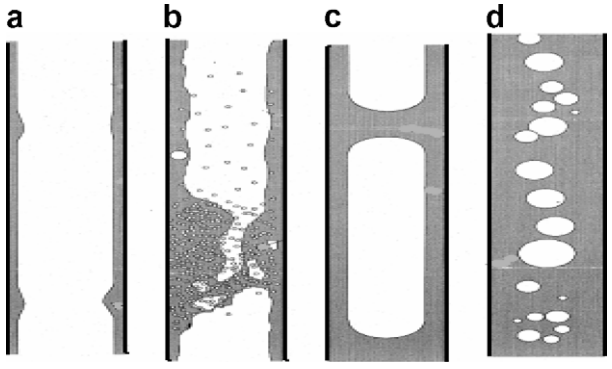

Fig. 1. Illustration of two-phase flow regimes in microgravity: (a) annular flow, (b) transition flow, (c) slug flow, and (d) bubbly flow.

3. Experiment

3.1. Purpose

Evaluate statistical parameters of void fraction measurements that can adequately identify the flow regime in microgravity.

3.2. Conceptual design

The normalized discrete probability density function (PDF), $p(x_j)$, is a function that satisfies the following properties: (1) The probability that x_j can take a specific value is $p(x_j)$, (2) $p(x_j)$ is non-negative for all real x_j, (3) The sum of $p(x_j)$ over all possible values of x_j is 1, that is

$$\sum_{j=1}^{N} p(x_j) = 1 \tag{1}$$

where j represents all possible values that x_j can assume and $p(x_j)$ is the probability at x_j.

Different statistical moments of the distribution have been analyzed to describe the shape of the PDF (Lewis and Orav, 1989). The four moments are the mean or the first moment about the origin, the variance or the second moment about the mean, the skewness or third moment about the mean, and the kurtosis or the fourth moment about the mean. The mean is the average of the distribution. When the distribution is arranged from the lowest to highest, the middle value is defined as the median. Variance is the measure of the dispersion of the population. Skewness is a measure of the asymmetry of a distribution. A positive skewed distribution will have a tail to the right side of the distribution while a negative skewed distribution will have a tail to the left side of the distribution. For a normal distribution the skewness is zero and the mean and median will be the same. Fig. 2 provides a visual depiction of the skewness where $\bar{\alpha}$ is the mean of the distribution.

The Kurtosis coefficient measures the peakedness of a distribution. Kurtosis is often compared with the peakedness of a normal distribution, called mesokurtic, which has a coefficient of kurtosis of zero. If the distribution is flatter than a normal distribution the coefficient of kurtosis is negative and it is called as platykurtic; if the distribution has more peakedness than a normal distribution the coefficient of kurtosis is positive and it is called as leptokurtic (Fig. 3).

An additional parameter useful for this investigation is the signal to noise ratio (SNR) defined as (see Fig. 4)

Fig. 2. Example of distribution with positive (left) and negative (right) skewness coefficients.

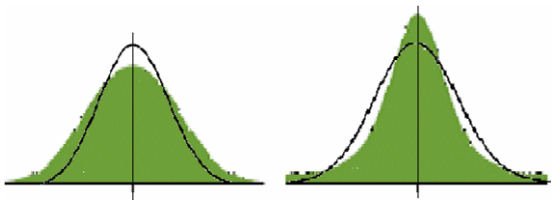

Fig. 3. Example of distribution with negative (left) and positive (right) kurtosis coefficient. The black line is the Gaussian distribution.

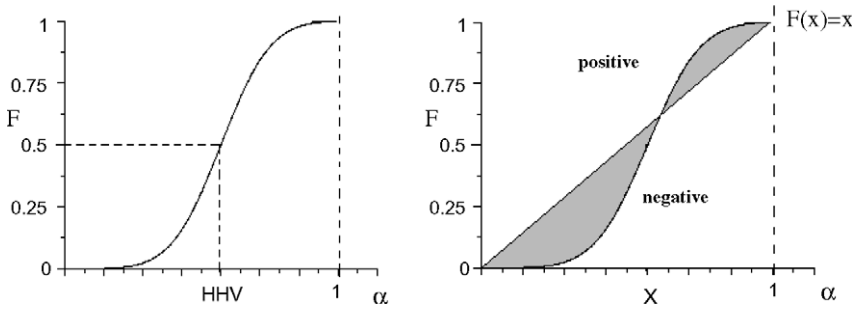

Fig. 4. Half height value (HHV) and linear area difference (LAD) examples for a simulated $F(x)$.

$$\mathrm{SNR} = \frac{\sigma^2}{\overline{X}} \tag{2}$$

where σ^2 is the variance and $\overline{X}$ is the mean. Another useful function is the discrete cumulative distribution function (CDF) defined as

$$F(x_j) = \sum_{i=0}^{j} p(x_i) \tag{3}$$

where $F(x)$ is the CDF and $p(x)$ is the normalized discrete PDF in x. The analysis of the shape of the CDF consists of the investigation of two parameters: the half height value (HHV) and the linear area difference (LAD). The HHV is defined as the value of α where the CDF assumes a value of 0.5

$$F(\mathrm{HHV}) = 0.5 \tag{4}$$

Another parameter is the linear area difference (LAD) that consists of the area between the line $F(x_j) = x_j$ and $F(x_j)$. Mathematically the two quantities are both non-dimensional. In formula

$$\mathrm{LAD} = \sum_{j=1}^{N} (F(x_j) - x_j) \tag{5}$$

where $F(x_j)$ is the CDF in x_j.

A brief description of how the parameters should behave for the different flow patterns and why this study considers them useful is presented below.

The variance is reasonably expected to be a flow pattern identifier. It is expected to be similar for bubbly and annular flow, while it should assume large values for slug flow because of the intermittent presence of the bullet shaped bubbles separated by regions of liquid slugs. The microgravity environment is expected to provide less variance due to the occurrence of smooth film annular flow and other distinct flow regimes that occur at lower volumetric flow rates in reduced gravity. Specifically, the reduction of the buoyancy effects is expected to result in a more stable flow pattern at lower flow rates.

The SNR is expected to have the same behavior as the variance but with a stronger trend because it consists of the variance weighted over the mean. This property will be more descriptive in the microgravity environment due to the characteristically smaller variances of the different flow regimes. The weighting of the mean should make the annular SNR very small (large void fraction, small variance); bubbly flows will have a large value for the SNR due to the small average void fraction in the denominator. Thus, the SNR provides a method of stretching the location of the different flow regimes through the use of the centering variable, the mean.

The coefficient of skewness should be positive (right tailed) for bubbly flow and negative (left tailed) for annular flow due to mostly liquid with few bubbles in the conduit for bubbly flow and almost all vapor with liquid layer for annular flow. In slug flow the PDF has bipolarity and so this coefficient has not a direct theoretical meaning but can be still useful and a negative value due to the left peak in the PDF is expected. In

particular the value of the skewness coefficient for slug flow is dependent on the relative length of the bullet shaped bubble.

The coefficient of kurtosis should be similar for annular and bubbly flow because the peakedness distribution is the same but with a different mean. Again there is no direct theoretical meaning in the case of slug flow because it is a measure of the peakedness and for a two-peak distribution no direct meaning is present and thus no relevant results are expected. The microgravity environment is expected to cause more peakedness compared to ground testing again because of the lower variance.

HHV and LAD are strongly correlated with the double peak of the PDF. HHV should increase from bubbly to annular flow while LAD should decrease from bubbly to annular. This happens because the slope of the CDF is greater for low values of void fraction for bubbly flow than for annular flow. Thus for annular flow the intercept for CDF equal to 0.5 is high (HHV high value) and the area below the straight line $F(\alpha) = \alpha$ assumes a large negative value (LAD negative). While for bubbly flow the intercept for the CDF equal to 0.5 is smaller than annular (HHV lower value) and the area below the straight line $F(\alpha) = \alpha$ is positive and large (LAD large).

3.3. Equipment

A complete description of the experimental setup is given by Hill and Best (1991), Reinarts (1993) and Hurlbert (2000). Fig. 5 shows a schematic of the flow loop.

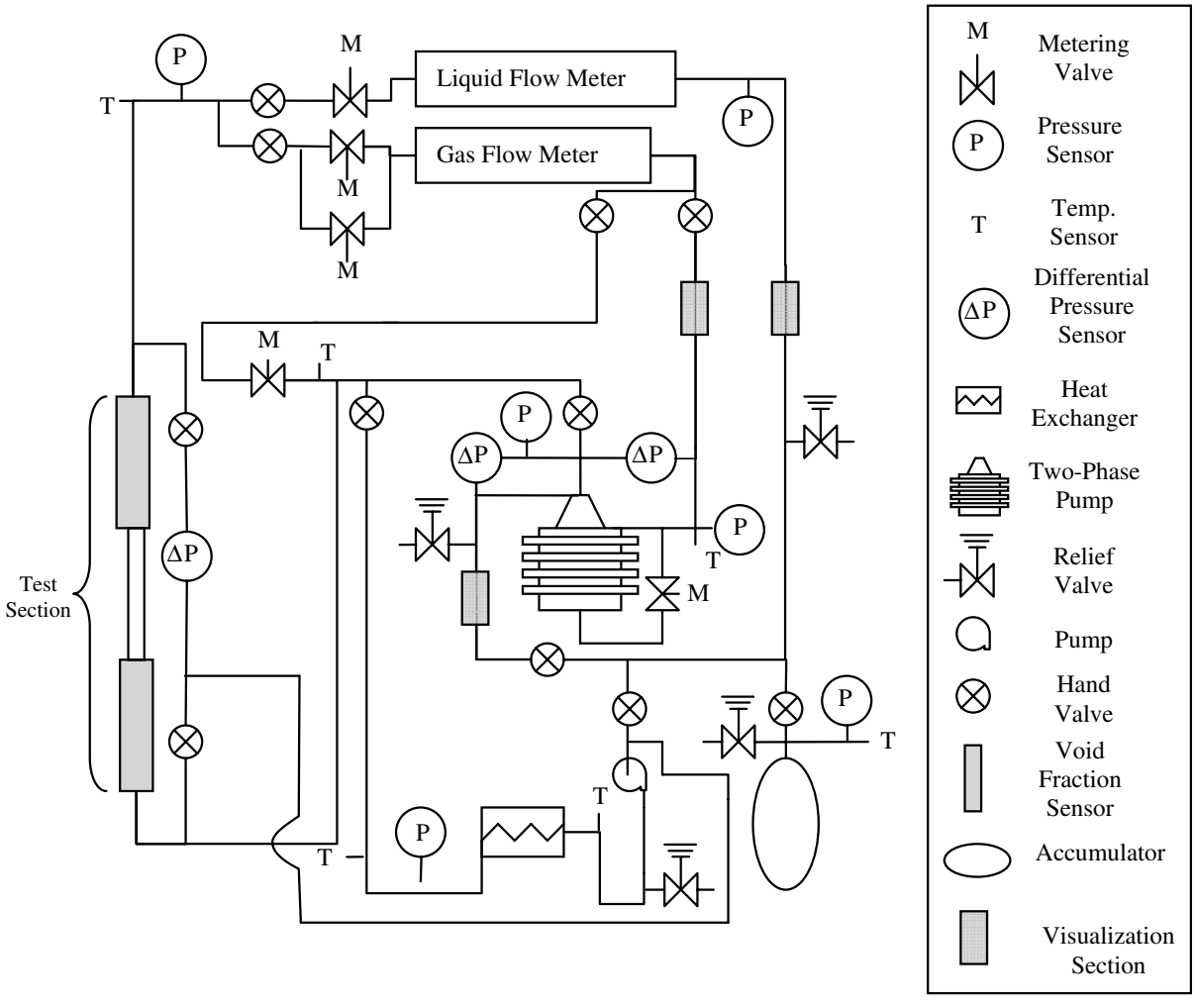

Fig. 5. Experiment configuration and instrumentation.

A Foster–Miller two-phase pump is a major component located at the center of the test bed. Two-phase flow enters the pump where the phases are first separated and then have their pressures increased. Each phase passes though a flow meter and metering valves prior to the mixing point before the development length. The development length consists of a 20 L/D tube followed by a CREARE void fraction probe, then a transparent visualization section and lastly a second CREARE void fraction probe. The clear section is Ultem pipe that allows flow visualization using a Kodak Ekta Pro high speed digital imager.

The instrument used to measure void fraction is an electrical capacitance probe made by CREARE Inc. and a complete description of the probe is given by Crowley et al. (1996) with validation under reduced gravity by Chang (1997). Developed for NASA, this probe is an inexpensive, non-nuclear, and accurate means to measure void fraction in two-phase thermal management systems and experiments under both steady-state and transient conditions. Notably, it is the only conductance-based void fraction instrument currently available for the measurement of dielectric fluids typically used for two-phase spacecraft systems and experiments.

The probe consists of three major components, a sensor spool, a printed circuit board, and a remote electronics box (Fig. 6). The sensor spool includes the end connections and housing compartment for the printed circuit board. The probe inner diameter is constructed to match the inner diameter of the system piping. Therefore, the sensor does not disturb the boundary layer of the flow. An array of sensors is placed inside the sensing spool. A Teflon lining is placed over the electrodes to protect the electrodes from the flowing fluid. In each sensor there are three void fraction measurement lengths: a 3 mm long ring, a 6.5 mm long ring and a 135 mm long volume-average sensor (Fig. 7). Crowley et al. concluded that the 3 mm and 135 mm sensors provide good measurements, while the 6.5 mm sensors show some problems of stability and so its measurements along with the volume averaged sensor were not considered. For this study, only the 3 mm sensor was considered since analysis of the instantaneous fluctuation of void fraction is desired. The capacitance sensor has an inner diameter of 12.7 mm (0.5 in.). The void fraction sensor output signals were collected at 100 Hz.

All testing was performed using R-12, dichlorodifluoromethane, as the working fluid. It was chosen for its low toxicity, low heat of vaporization, and material compatibility properties and in particular for its high vapor density at low pressure. The facility operates at a temperature of about 295 K. The corresponding sat-

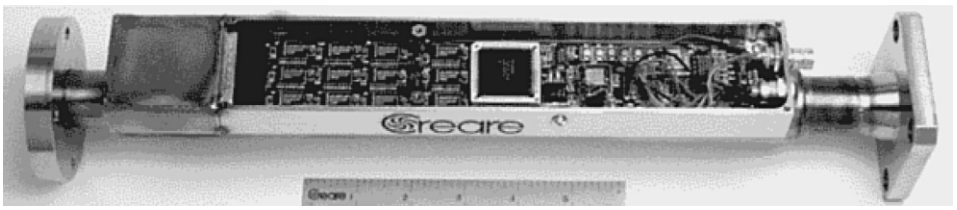

Fig. 6. CREARE Inc. void fraction sensor.

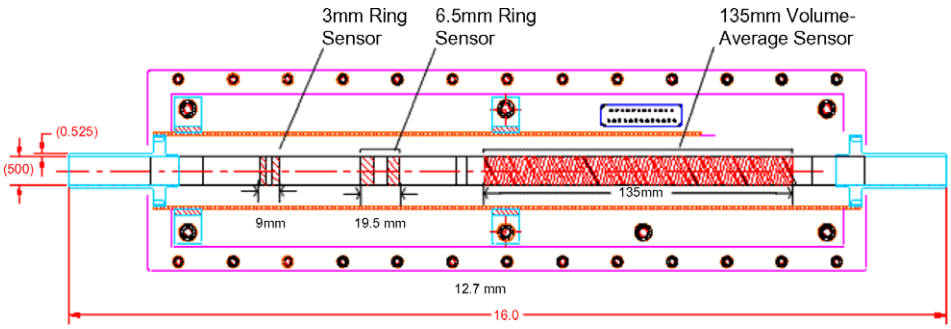

Fig. 7. CREARE Inc. void fraction sensor's sensor rings.

uration pressure is about 600 kPa. The experiment was flown aboard the NASA-Johnson Space Center (JSC) KC-135 aircraft stationed at Ellington Field in Houston, Texas. The KC-135 airplane flies alternating periods of high gravity (~1.8 g) and reduced gravity (~0 g) for 20 s by flying a parabolic path.

4. Results and analysis

The superficial vapor velocity ranged from 10 cm/s to 300 cm/s and the superficial liquid velocity ranged from 1 cm/s to 30 cm/s. Most of the two-phase data collected for this experiment were observed to be in the slug and annular regions based on a review of the high speed imagery.

4.1. Data observations and analysis

The data shown in Fig. 8 have been classified based on visual observation of high speed imagery and are plotted as superficial vapor velocity vs. superficial liquid velocity. Also shown in Fig. 8, is Creare's predicted flow regime transition between the slug and annular flow regimes. It should be noted that the visual observations are consistent with that of Vince and Lahey (1982) but inconsistent with those of Crowley et al. (1996) and Kurwitz and Best (2002). This reinforces the need for a quantitative technique to identify flow regimes.

The following are graph sets consisting of (a) a high speed digital image that shows the flow regime under observation, (b) a graph of void fraction vs. time, (c) the corresponding probability density function, and (d) cumulative density function graphs. Each graph set is for a particular flow regime. Figs. 9–11 show the graph sets for the three considered flow regimes: annular, transition, and slug flow.

4.2. Statistical analysis

4.2.1. Variance

The variance values plotted in Fig. 12 were determined from the PDF plot values shown in Figs. 9c, 10c, and 11c. Fig. 12 shows variance as a function of void fraction. Notice the regions of dominance of the different flow regimes, an indication of the viability of variance as a flow regime identifier.

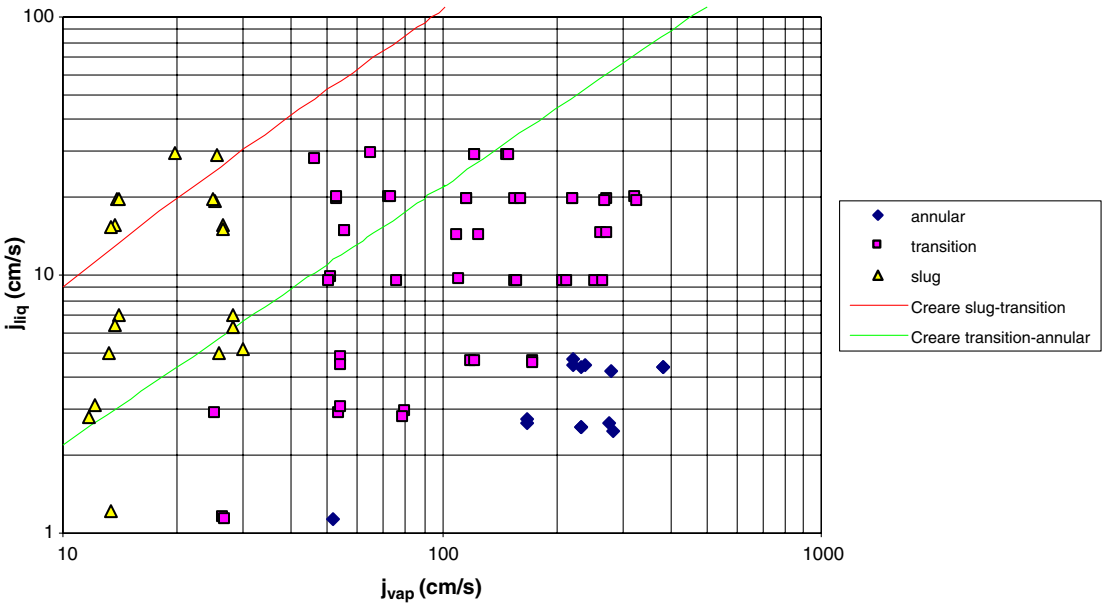

Fig. 8. Plot of superficial phase velocities used in the present experiment, the corresponding observed flow regimes, and comparison of the predicted flow regime transition lines (CREARE model) with the actual flow regime transitions.

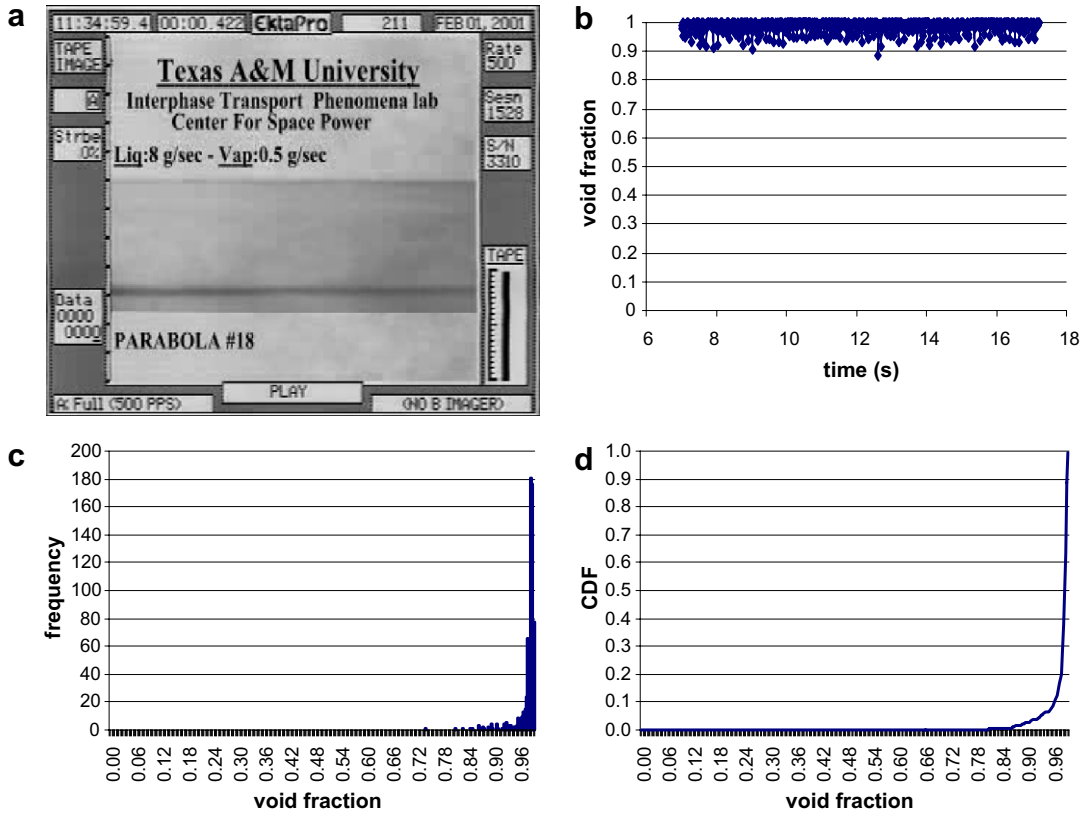

Fig. 9. Graph set for annular flow; $j_{vapor} = 51.44$ cm/s, $j_{liquid} = 1.14$ cm/s: (a) picture, (b) void fraction vs. time, (c) PDF, and (d) CDF.

The graph is divided into three regions corresponding to the three observed flow regimes. From the variance range of 0–0.0005, annular flow exists. From 0.0005 to 0.027, transition flow and at greater than 0.027, slug flow. The variance values range from its minimum in the annular flow region through the transition region to its maximum in the slug flow region. This is explained by the fact that in the slug region, intermittent patterns of liquid-bubble, liquid-bubble produce a value of variance that is higher than the annular region where the surface is smooth resulting in a constant void fraction. Some slug points are in the transition area because the long bullet shaped bubbles produce a region of lower variances (quasi-annular).

The spread of the slug flow data points is attributed to the various sizes of the Taylor (bullet-shaped) bubbles. The result for void fraction values 0.6–1 is in accordance with the Vince and Lahey (1982) experiments. Different values have been found for smaller void fraction (from 0.4 to 0.6, in the slug region) due to the fact, as said before, they have a strong relation with the slug configuration.

It is expected that the variance for annular flow in microgravity is smaller than in earth-gravity conditions. This is due to the absence of body forces; thus the annular regime can be achieved with smaller superficial velocities in microgravity; hence the gas–liquid shear is reduced and the interface smoother.

4.2.2. Signal-to-noise ratio (SNR)

Using Eq. (5), the signal-to-noise ratio is computed and plotted in Fig. 13.

SNR achieved the same data shape as the variance. Three regions could be identified for the SNR: from 0 to 0.0005, annular flow exists; from 0.0005 to 0.02, transition; and more than 0.02, slug flow.

4.2.3. Skewness

Fig. 14 plots skewness as a function of void fraction.

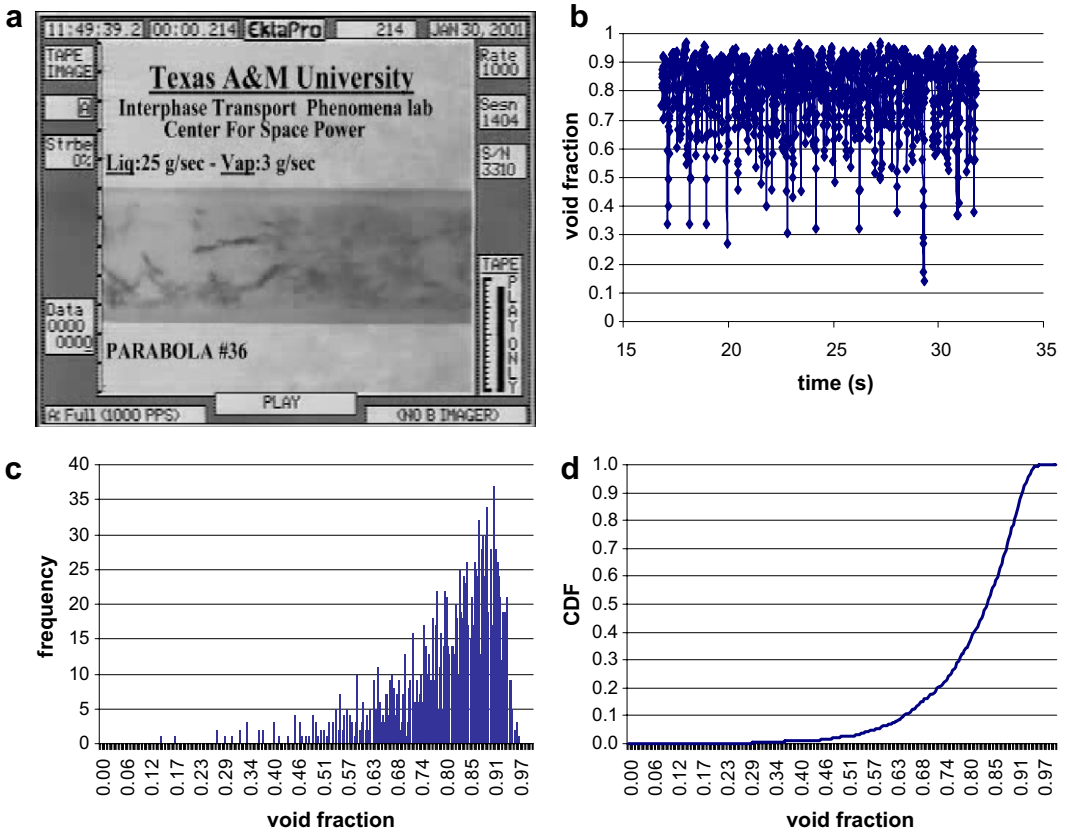

Fig. 10. Graph set for transition flow; $j_{vapor} = 46.19$ cm/s, $j_{liquid} = 28.15$ cm/s: (a) picture, (b) void fraction vs. time, (c) PDF, and (d) CDF.

A positive skewness coefficient means a right-tailed distribution and a negative means a left-tailed distribution. An interesting observation from Fig. 14 is that in general, slug flow has a smaller skewness coefficient than transition flow for the same void fraction values. This is reasonable because the two-peak slug distribution consists of a more left-tailed PDF shape. Additionally, annular flow assumes small skewness coefficient values because the distribution does not present any left tail.

The values of the variance and skewness for annular and transition flows are similar to the work presented by Vince and Lahey (1982). The values of the skewness coefficient are different due to a slightly different theoretical definition of the statistical moment but the trend (not the scale) is similar. The present work and Vince–Lahey both have a skewness minimum for a void fraction equal to 0.8–0.9. Moreover Vince–Lahey's skewness goes to zero around a void of 0.4. The unique categorization due to the complexity and the inaccuracy of this parameter results in a more complicated identification than variance and SNR.

4.2.4. Kurtosis

The plot in Fig. 15 shows the coefficient of Kurtosis.

This parameter fails the requirements to be a valid flow pattern identifier. Vince and Lahey (1982) found a different distribution. The discrepancy between the data of the two studies could be explained in different ways, most likely, the small variation due to inaccuracy in the measurements resulted in a large disparity in the void fraction values that was further magnified by the Kurtosis coefficient being a fourth order statistical moment.

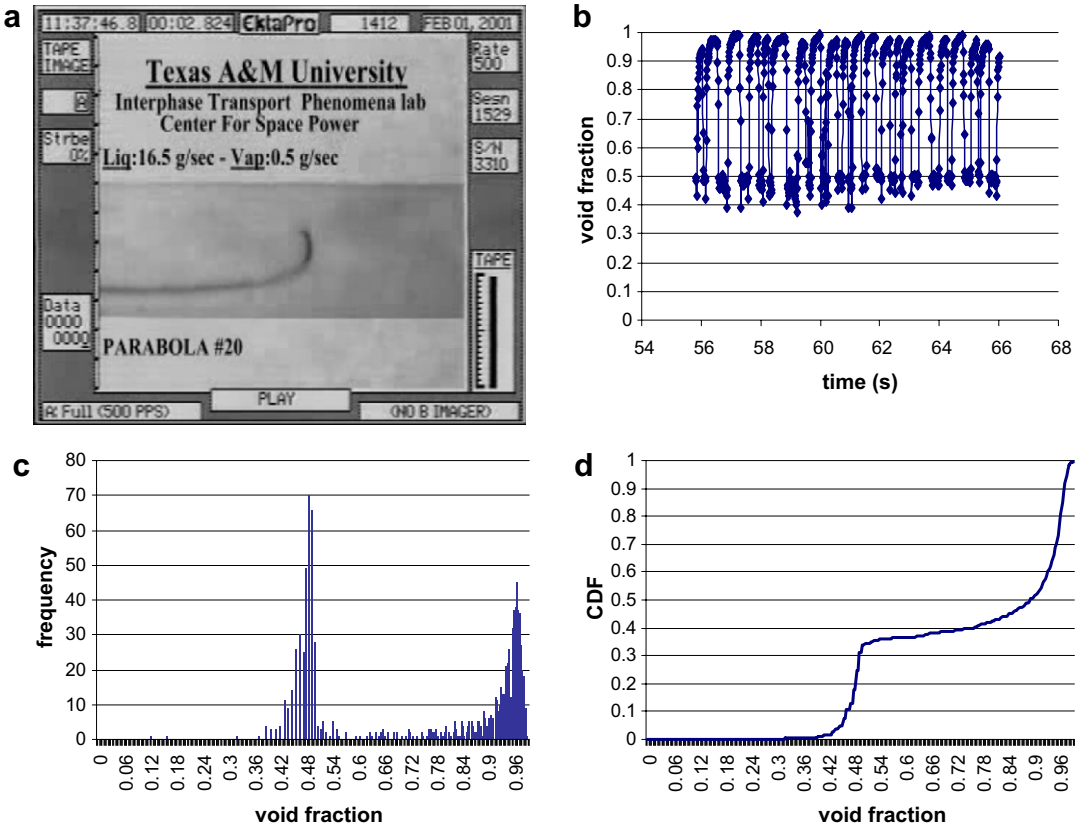

Fig. 11. Graph set for slug flow; $j_{vapor} = 19.20$ cm/s, $j_{liquid} = 20.97$ cm/s: (a) picture, (b) void fraction vs. time, (c) PDF, and (d) CDF.

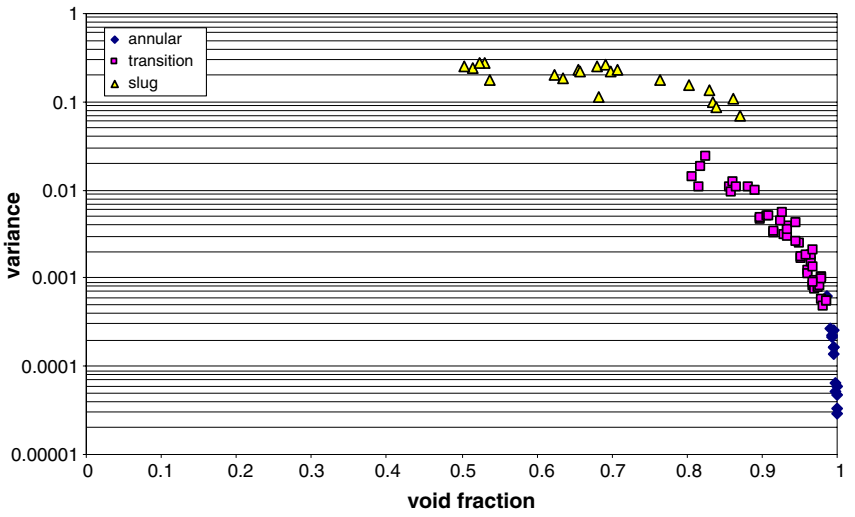

Fig. 12. Variance as a function of void fraction.

4.2.5. Half height value (HHV)

Fig. 16 illustrates the value of the HHV as function of the average void fraction computed from Eq. (4).

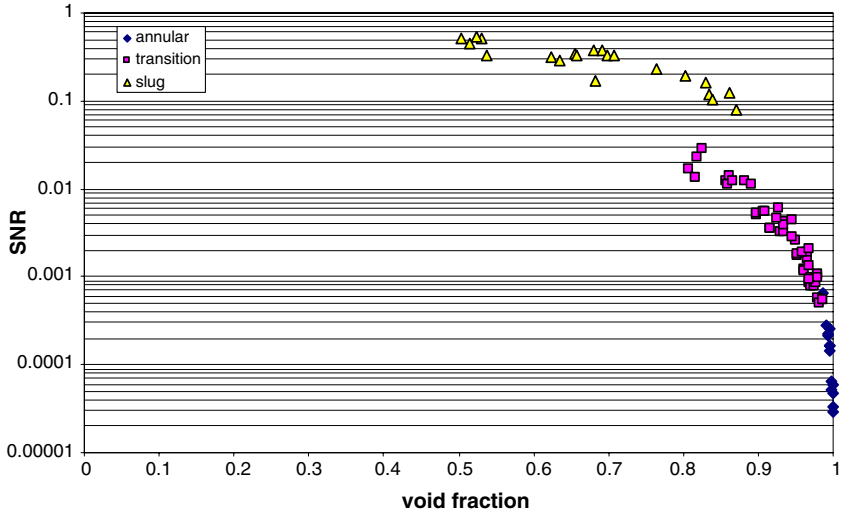

Fig. 13. SNR as function of void fraction.

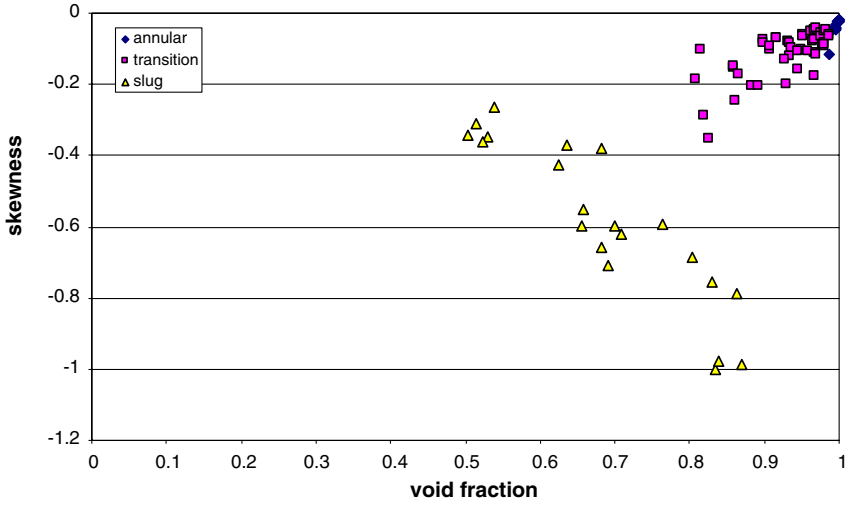

Fig. 14. Skewness coefficient as a function of void fraction.

The results for HHV are in perfect accordance with expectations. Fig. 16 presents high values for annular flow (from HHV = 0.998 to HHV = 0.999) because the CDF presents only a single strong peak at high void fraction values.

HHV for slug flow is out of the transition-annular trend line and assumes larger values. In addition, for equal values of the void fraction HHV is greater for slug than for transition flow. This is due to the presence of the left peak in the slug distribution that moves the CDF left.

The plot in Fig. 16 could be a good flow pattern identifier. Annular and transition flow are in an almost linear correlation while slug has a scattered behavior. As mentioned before this is due to the variability of the slugs, in particular with the length of the bullet shaped bubbles.

4.2.6. Linear area difference (LAD)

From Eq. (5), the LAD is computed and plotted in Fig. 17. Annular flow has a very negative LAD value because annular flow only assumes high void fraction values. Furthermore, slug flow is outside of the

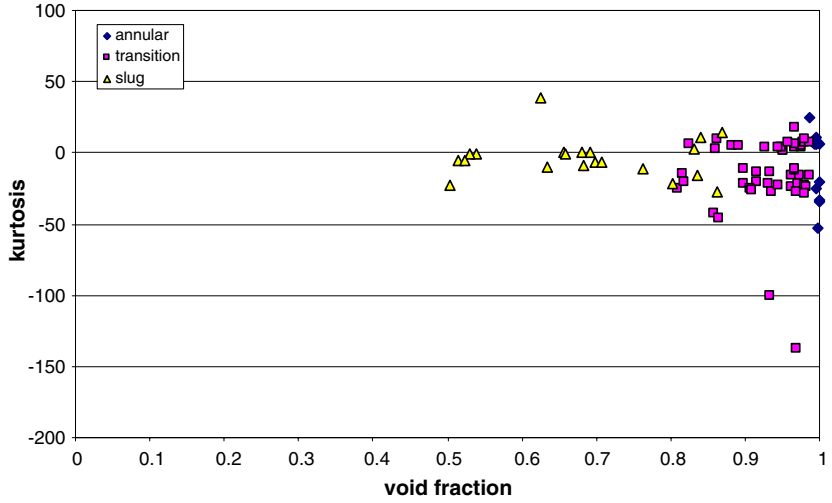

Fig. 15. Kurtosis coefficient as a function of void fraction.

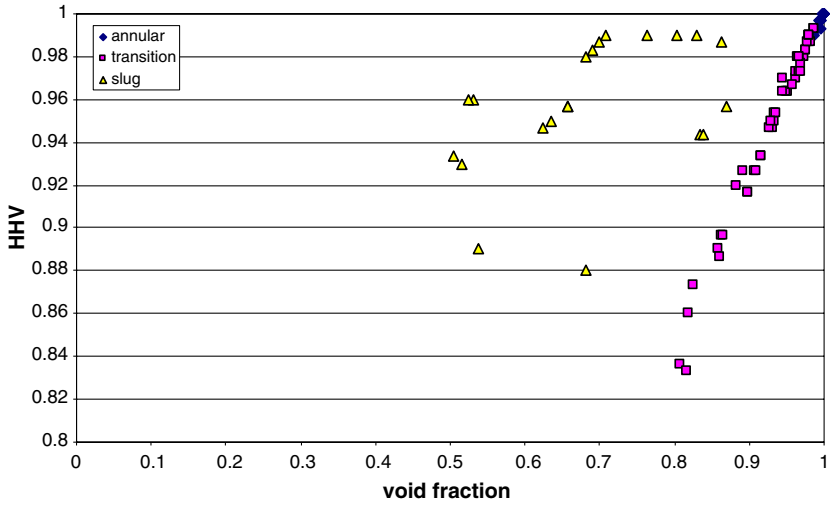

Fig. 16. HHV as function of void fraction.

transition and annular line. In fact, the slug LAD is smaller than the transition LAD for equal void fraction values because the CDF is flat for middle values. This happens because in slug flow few points with a void fraction between the one of annular and full water were detected. Transition values sit on an almost linear trend line ($R^2 = 0.9998$ for first campaign and $R^2 = 0.8605$ for the second). The reason is that the transition flow PDF distributions have almost the same shape for different void fractions. The same shape for different void fraction means that the area is strictly dependent on the averaged void fraction. The graph in Fig. 17 could helpful for flow pattern identification.

The HHV and LAD have shown a good capability to indicate different flow patterns and in particular to distinguish and describe the two-peak distribution of slug flow from the others. These approaches are more versatile than the other flow regime indicators because they can be easily applied to both analytical functions and experimental data.

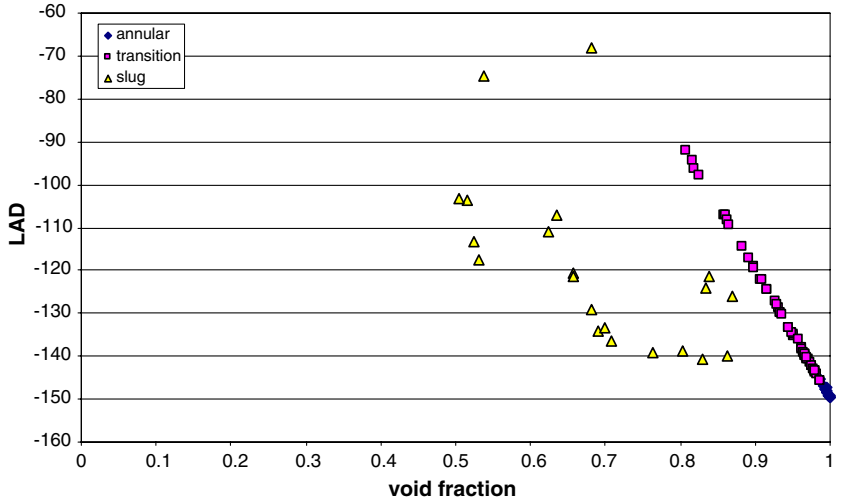

Fig. 17. LAD as a function of void fraction.

5. Conclusions

The purpose of this study was to determine if statistical parameters evolved from void fraction fluctuation measurements could be used to identify the flow regimes in the microgravity environment. The results show that the variance and SNR are good flow regime identifiers (larger values for slug and smaller values for annular). The skewness coefficient was found in accordance with similar past experiments and is still not useful for flow regime identification. The Kurtosis coefficient data were different from past experiments and did not present any relevant characteristic properties. The HHV and the LAD are useful for the identification of the annular region and show a clear linear trend in the transition and annular regions while outlier behavior identifies the slug flow region.

Reduced gravity experiments are expensive and difficult to perform resulting in a limited database for reduced gravity two-phase flow. It is imperative that a technique to allow accurate classification of flow regime for different experiments allowing analysis with a composite data set. The requirement to minimize mass, volume, and power in spacecraft, requires that systems be able to operate across different flow regimes. Furthermore, the preceding requirements drive interest in lower superficial velocities where one must consider other forces such as surface tension rather than inertial effects.

This experiment proposes a universal definition of flow regime, dependent on the single parameter of the statistical variance of the void fraction measurement. Extending this definition into application, flow regime measurement has become realistic with the technological arrival of a high accuracy, high sampling rate, and non-interfering sensor such as the CREARE, Inc. void fraction probe. Utilization of this newly available technology and methodology can dramatically improve systems dependent on flow regime information, making them accurate, real-time, and non-impacting. Conclusively, the techniques demonstrated in this experiment verify the use of statistical analysis on void fraction measurements to identify flow regimes in microgravity.

Acknowledgements

This study was carried out with resources provided by CREARE Inc. and the NASA Center for Space Power Grant. The authors also thank Katy and Yantee.

References

Chang, J. H., 1997. Statistical Comparison of Void Fraction Instrumentation in Microgravity Environment. M.S. Thesis, Texas A&M University, Department Nuclear Engineering, College Station, TX.

Crowley, C.J., Magari, P.J., Martin, C.M., Hill, M.E., 1996. A void fraction instrument for two-phase flow in dielectric liquids. In: Proceedings of the 34th Aerospace Sciences Meeting & Exhibit, Reno, Nevada, AIAA-96-0925.

Elbow, K.J., Rezkallah, K.S., 1997. Statistical analysis of void fluctuation in gas–liquid flows under 1-g and μ-g conditions using a capacitance sensor. Int. J. Multiphase Flow 23, 833–844.

Hill, W.S., Best, F.R., 1991. Definition of Two-Phase Flow Behaviors for Spacecraft Design, PL-TR 91-1050, Phillips Laboratory.

Hurlbert, K.M., 2000. Flow Dynamics for Two-Phase Flows in Partial Gravities. PhD Dissertation, University of Houston, Houston, TX.

Janicot, A., Dukler, A.E., 1993. A model for gas–liquid flow at reduced gravity conditions. AIChE J. 39, 1101–1106.

Jones Jr., O.C., Zuber, N., 1975. The interrelation between void fraction fluctuations and flow patterns in two-phase flow. Int. J. Multiphase Flow 2, 273–306.

Kurwitz, R.C., Best, F.R., 2002. New results in gravity dependent two-phase flow regime mapping. In: Proceedings of the Conference on Applications of Thermophysics in Microgravity and Breakthrough Propulsion Physics, Albuquerque New Mexico, 2-2002.

Lewis, P.A.W., Orav, E.J., 1989. Simulation Methodology for Statisticians, Operations Analysts, and Engineers. Wadsworth & Brooks/Cole Advanced Books & Software, Pacific Grove, CA.

Lowe, D.C., Rezkallah, K.S., 1999. Flow regime identification in microgravity two-phase flow using void fraction signal. Int. J. Multiphase Flow 25, 433–457.

Reinarts, T.G., 1993. Adiabatic Two Phase Flow Regime Data and Modeling for Zero and Reduced (Horizontal Flow) Acceleration Field. PhD Dissertation, Texas A&M University, College Station, TX.

Vince, M.A., Lahey Jr., R.T., 1982. On the development of an objective flow regime indicator. Int. J. Multiphase Flow 8, 93–124.